TÉCNICO LISBOA

Distributed Real Time Control Systems

Autores:
Rodrigo Coimbra: 100078

1 Introduction

Modern office environments often face challenges in maintaining optimal lighting conditions throughout the day. The conventional static lighting systems fail to adapt to the dynamic changes in natural light and occupancy, resulting in inefficient energy usage and suboptimal illumination levels.

This project focuses on implementing a control system designed to dynamically adjust the lighting levels of a single luminaire for optimal illumination while prioritizing energy efficiency. The objective is to enhance user comfort by delivering the appropriate amount of light when needed, while minimizing energy.

2 System

The office illumination system will be simulated inside a shoebox, shown in figure 1, where we have three luminaries, each with its own LED driving circuit and an illuminance reading circuit. Additionally, each luminaire is equipped with a Raspberry Pi Pico (RPI Pico) to control its system.

(a) Inside

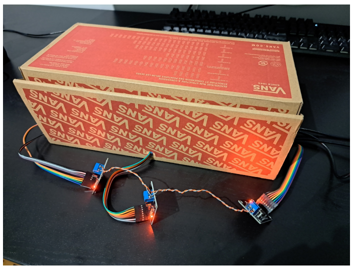

(b) Outside

Figure 1: BOX

2.1 LED Driving Circuit

As can be seen in figure 2a, each LED is controlled via PWM, influencing the power of luminaire proportionally. Furthermore, a linear relationship exists between the luminaire powers and the measured illuminances, allowing us to establish the equation 1, under the assumptions that the light propagation in air is very fast and that the external illuminance within the box is zero.

$$x(t) = Gu(t) + o(t) \xrightarrow{o(t)\to 0} G^{-1}x(t) = u(t) \tag{1}$$

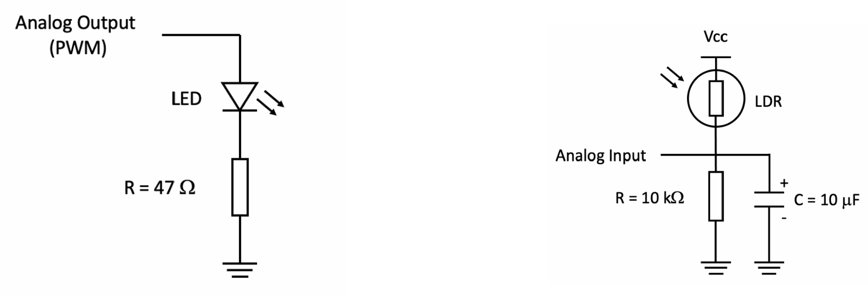

(a) Led Driving Circuit **(b)** Illuminance reading circuit

Figure 2

This equation provides a reliable approximation of the duty cycle to be used for the LED, given a reference Lux level, in a system that hasn't any type of disturbance, including other LEDs inside the box. Furthermore, it operates independently of the actual illuminance incident upon the system, therefore, providing a feedforward value for the duty cycle, denoted as u_{ff}.

Despite being a good approximation for a system without disturbances, we must adapt our system to accommodate all scenarios. Therefore, we need to introduce some feedback into our system.

2.2 The Illuminance Measurement System (Luxmeter)

To accurately adjust the light to a specific reference level, we need to first measure it. To achieve this, we employed the circuit shown in figure 2b.

The Light Dependent Resistor (LDR) is a nonlinear element, however its relationship to LUX demonstrates an affine relationship in the log-log scale. This relationship is described by

$$\log_{10}(LDR) = m\log_{10}(LUX) + b \Leftrightarrow LUX = 10^{\frac{\log_{10}(LDR)-b}{m}} \tag{2}$$

$$b = \log_{10}(LDR) - m\log_{10}(LUX) \tag{3}$$

This model of the LDR has a resistance of $150k\Omega \sim 300k\Omega$ when exposed to 10 Lux of illuminance[1]. Therefore, due to the lack of a proper device to adjust the resistance to a 10 LUX illuminance, we assumed a median value, $225k\Omega$, for that same illuminance. Additionally, we can observe the sensitivity value, $\gamma = 0.8 \pm 0.1$[1].

With these values, we can calculate m and b, which are $m = -0.8 \pm 0.1$ and $b = \log_{10}(225000) - m$, respectively, when substituting the values in equation 3. Furthermore, due to the affine relationship of equation 2, we will fine-tune the m to each luminaire later in this report.

To compute the value of LUX in the system (equation 2), we still miss the value of the LDR at each sample, and therefore, we need to calculate it.

To compute the LDR, we can derive it from the formula of a voltage divider, resulting in the following

$$V_{ADC} = VCC\frac{R}{R+LDR} \Leftrightarrow LDR = \frac{VCC \cdot R}{V_{ADC}} - R \tag{4}$$

Where R is the $10k\Omega$ and V_{ADC} is the voltage at the Analog input in the figure 2b.

[1] LDR spreadsheet

Finally, we read our input using an Analog-to-Digital Converter (ADC), and we need to convert it to voltage to use it in Equation 4. The resolution of our ADC is 12 bits. To convert this reading to volts, we multiply the value read by $\frac{VCC}{(2^{12}-1)} \Rightarrow \frac{3.3}{4095}$.

To minimize noise as much as possible, we incorporate a capacitor in parallel to filter out high frequency values that the LDR may detect due to the nature of PWM operation. This occurs because, despite having the maximum frequency of 60 kHz available for PWM, the LED is turned off for a portion of the cycle. Additionally, a digital filter was implemented, i.e., the analog input is sampled 20 times, and then the mean of these readings is calculated to determine the LUX value.

2.3 Gain

As observed previously, adjusting the duty cycle of the LED allows us to linearly change the system's LUX output. Therefore, by varying the duty cycle value and measuring the LUX after the system reaches a steady state, we can compute the gain of the system, which will be its slope. This process was repeated for fourteen values to ensure that the slope remains constant.

By utilizing the previously determined value of $m = -0.8$, we obtain the orange dots depicted in figure 3a. When comparing these dots to the linear regression line that best fits them, it becomes evident that these points deviate from the linear regression line (orange line), which ideally should represent the linear gain of the system. Consequently, we should explore other values within the specifications to determine if they establish a closer alignment between the points and the regression line.

Given that the uncertainty of m is ± 0.1, data was collected within the range of $m = -0.7$ to $m = -0.9$ with a step size of 0.01. Then, the slope between points was calculated and normalized, and subsequently, the sum of squared errors (SSE) was calculated. The results are presented in table 1. Therefore, we conclude that the best value of $m = -0.89$ (figure 3b), and consequently, $b = log(225000) + 0.89$ (equation 3).

m	-0.7	-0.8	-0.89	-0.9
SSE	1.7956	0.9200	0.2969	0.3925

Table 1: SSE of gains to different values of m

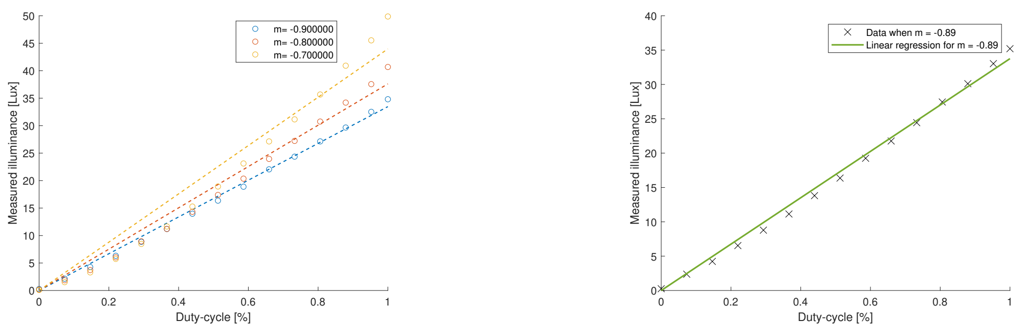

(a) Using the full range of m

(b) Final value of m

Figure 3: Fine-tune of m

After determining the optimal values for m and b, we have established an almost linear relationship between the duty cycle and the illuminance measured by our system. To maximize the accuracy of our system overall, during initialization, it measures the illuminance both with the luminaires off (duty cycle 0) and on (duty cycle 1). The resulting slope is then considered the static gain of the system.

2.4 Tau

In our system, τ characterizes the response time of the system to some input, representing the time required for the system's response to reach approximately 63% of the change from the initial value to the final value. This can be computed theoretically using the equation 5, where R and C represent the resistance and capacitance, respectively, represented in the figure 2b respectively. Figure 4a show a plot of the theoretically $\tau(LUX)$.

$$\tau = R_{eq}C \Leftrightarrow \tau = \frac{LDR \cdot R}{LDR + R}C \tag{5}$$

Additionally, the value of τ in our system can be measured experimentally, resulting in the figures 4b and 4c. More values of τ are represented in the table 2.

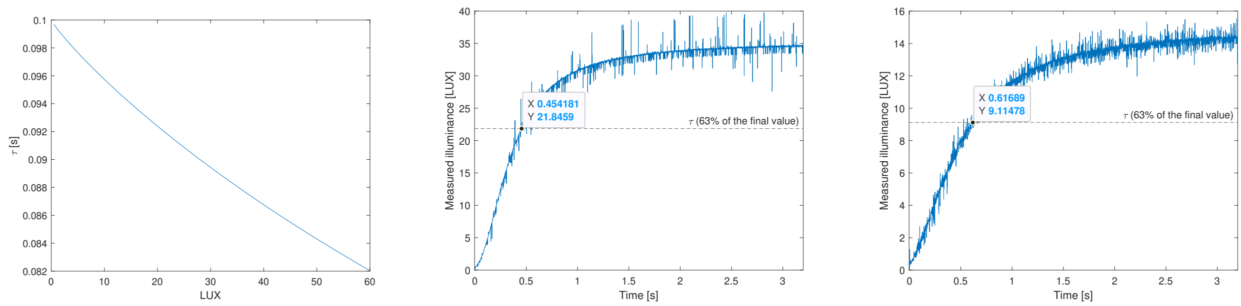

(a) Theoretical τ **(b)** Response to 1 Duty Cycle Step **(c)** Response to 0.5 Duty Cycle Step

Figure 4

Initial Duty Cycle of the LED	0	0	0	0.5
Final Duty Cycle of the LED	1	0.5	0.25	1
τ [s]	0.454	0.617	0.747	0.144

Table 2: Values of *tau* to different steps

From this experiment, we can conclude that despite following the trend of larger values of illuminance leading to smaller values of τ, the actual values are somewhat different from what we expected theoretically. One possible reason for this variance is that the theoretical calculation assumes an instantaneous change in the LDR with illuminance, whereas in reality, the LDR takes some time to adapt to changes in illuminance.

3 Controller

To control the luminaries of the given system, a set-point weighting PID controller was chosen. However, since this system has no inertia, the derivative term is not needed. Therefore, the term that specifically control it was set to 0 ($T_d = 0$), resulting in a set point weighting PI controller. This system is represented in figure 5.

In this PI controller, the final output is the summation of two terms: the proportional (P) and integral (I) terms (equation 8). The original formulas for these terms consider a continuous input, however, since our system is a digital controller, it receives discrete inputs rather than continuous ones. Therefore, the formulas were discretized, as demonstrated in equations 6 and 7. Additionally, a constant sample time, h, of $10ms$ was chosen for consistency between samples and efficiency in the control process.

$$P(t) = K(bv_{ref}(t) - y(t)) \xrightarrow{Discretization} P(t_i) = K(bv_{ref}(t_i) - y(t_i)) \tag{6}$$

$$I(t) = \frac{K}{T_i}\int_0^t (v_{ref}(s) - y(s))\, ds \xrightarrow{Discretization} I(t_{i+1}) = \frac{Kh}{Ti}(v_{ref}(t_i) - y(t_i)) \tag{7}$$

$$u(t_i) = P(t_i) + I(t_i) \tag{8}$$

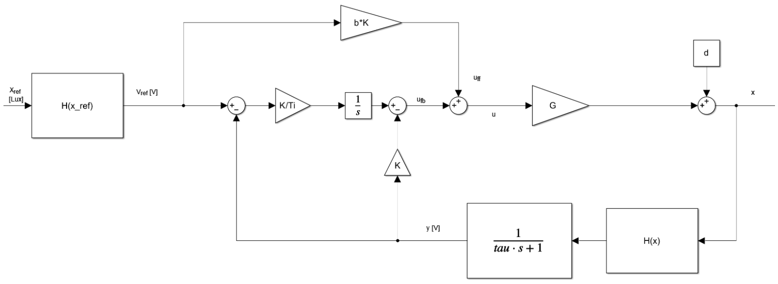

Figure 5: Initial controller

3.1 Parameters and Transfer function

The set point weighting PI controller implemented in this project can be described by the following transfer function

$$\frac{X}{X_{ref}} = \frac{(bT_i s + 1)(s\tau + 1)}{(s\tau + 1)\frac{T_i s}{GHK} + T_i s + 1} \tag{9}$$

As we aim for the LED to quickly follow the reference without overshoots or oscillations, the ideal transfer function would be the identity.

$$1 = \frac{(bT_i s + 1)(s\tau + 1)}{(s\tau + 1)\frac{T_i s}{GHK} + T_i s + 1} \Leftrightarrow$$
$$\frac{T_i s}{GHK} + \frac{T_i s + 1}{s\tau + 1} = bT_i s + 1 \rightarrow$$
$$\xrightarrow{T_i = \tau} \frac{s\tau}{GHK} + \frac{s\tau + 1}{s\tau + 1} = bs\tau + 1 \Leftrightarrow$$
$$1 = GHKb \Leftrightarrow b = \frac{1}{GHK}$$

By solving equation 3.1, we discovered good approximations for $T_i = \tau$ and $b = \frac{1}{GHK}$. Additionally, values for τ, H and G have already been computed, leaving only the value of K to be determined. The value of K will influence the response time of the system to disturbances. Since we aim for a slow reaction to disturbances, we require a small value for K.

3.2 Improvements to the base controller

Due to system constraints, there may be cases where we cannot follow the reference level. This is because our LED, even at maximum output, only reaches approximately 35 LUX. Consequently, if our reference exceeds this level, the integrator will continue to accumulate the error between that reference and the maximum output of the LED. Similarly, if the reference falls below the external illuminance, the integrator will still register an error even if the LED is turned off.

These issues can result in slow response times. To address this, we implement an anti-windup mechanism, allowing us to control the integral term as follows

$$I = I + \frac{Kh}{T_i}(v_{ref} - y) + \frac{h}{T_t}(u - v) \tag{10}$$

where u is the value saturated within the LED's operational limits and v is the value before being limited.

Since u is limited, as v goes beyond the limits, it will begin to restrict the integral term (using equation 10), increasing the restriction as the absolute difference between u and v increases. If v is within the limits, then v and u will have the same value, and consequently, anti-windup will not affect the output. Implementing this we obtain the system represented in the figure 6

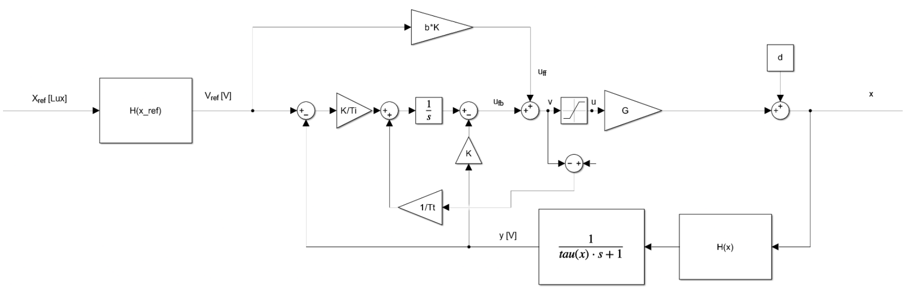

Figure 6: System with Anti-Windup

Another improvement made, was implementing a bumpless transfer method, allowing us to change the K and b parameters without causing any sudden changes in the illuminance of the system. To achieve that we calculated the new value of the integral term using the equation 11.

$$I_{new} = I_{old} + K_{old}(b_{old}v_{ref} - y) - K_{new}(b_{new}v_{ref} - y) \tag{11}$$

4 Simulator

The PI controller was then simulated in Simulink (Matlab) using the schematic shown in figure 7. To better simulate a real scenario a disturbance similar to the ambient light was added at the end (random values from a Gaussian distribution with $\mu = 0.28$ and $\sigma = 0.001$). The best parameters found after a fine-tune are the ones presented in the Table 3. The results to some steps are represented in figure 8a, where the blue line is the reference signal and the yellow line is the measured LUX at each instant. The τ consider was the mean of the table 2.

The simulator was also tested on its system of anti-windup. To do that, the same disturbance used before was applied, but this time with a $\mu = 14$. As can be seen in figure 8b, even after a while with a reference that its unachievable, it quickly responds to a change to a reference that it can reach.

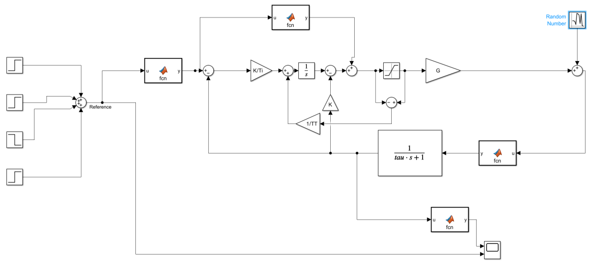

Figure 7: Simulink simulator

h [s]	K	G [LUX/dc]	T_i [s]	T_t [s]	H [Volt/LUX]	b	tau [s]
0.01	0.8	32.77	0.5	1.5	$\frac{v_{ref}}{x_{ref}}$	$\frac{1}{KGH}$	0.5

Table 3: Parameters of the simulator

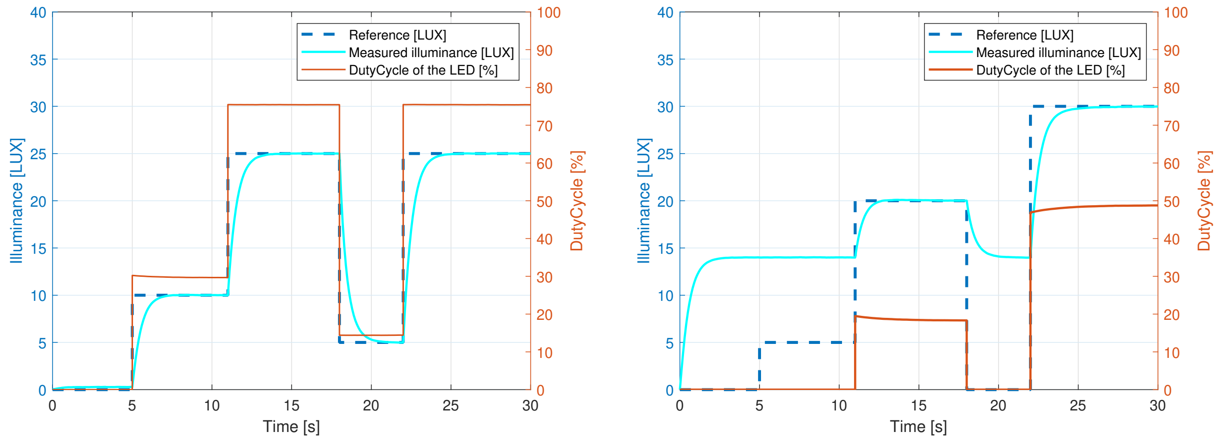

(a) Response to changes of reference **(b)** Test of the anti-windup on the simulator

Figure 8: Simulator

5 Results

When testing our real system with the same parameters used in the simulation (Table 3), we obtain the figure 9a. As we can see, those parameters were not the best possible, resulting in responses not ideal. Therefore, the parameters were fine tuned, resulting in the parameters presented in the Table 4 and in the figure 9b.

h [s]	K	G [LUX/dc]	T_i [s]	T_t [s]	H [Volt/LUX]	b
0.01	0.15	32.77	$\tau_{theoretical}(x_{ref})$	1.5	$\frac{v_{ref}}{x_{ref}}$	$\frac{1}{KGH}$

Table 4: Parameters of the real system

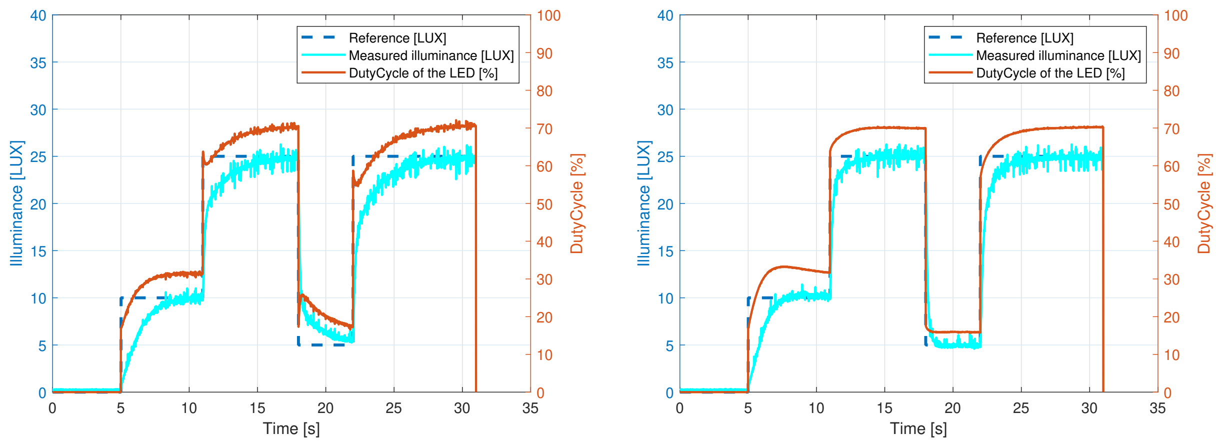

(a) Same parameters of the simulator **(b)** Fine tuned parameters

Figure 9: Response to changes of reference

5.1 Can Bus

In this first half of the project we started working with the can bus that will play a major role on the second half of the project, because they allow the RPI Pico to communicate between them. In this case, we sent a message from our RPI Pico to the other two and received a message from both as well (figure 10).

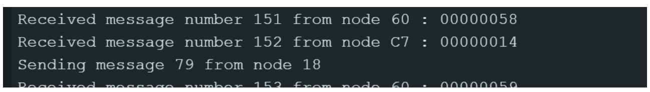

Figure 10: RPI Pico communicating using the can bus

5.2 Anti-Windup and Bumpless transfer

To improve this PID controller, two methods were used. The first one, used when the LED cannot reach the reference within its limitations, therefore, it limits and control the integrator parameter of the PID. The difference on this system with this mechanism working and not working can be seen in the figure 11a Additionally, to smoothly transition between different parameters of K and b, a bumpless transfer method was implemented. The results of this mechanism working are represented in 11b.

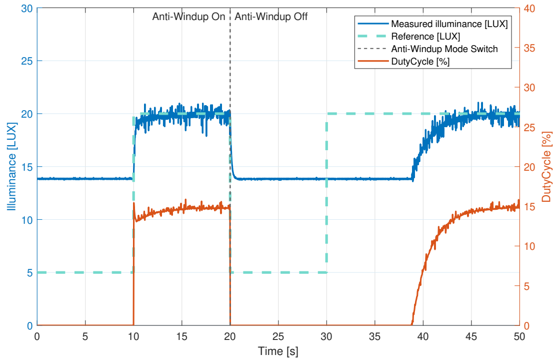

(a) Anti-windup results (Left - ON / Right - OFF)

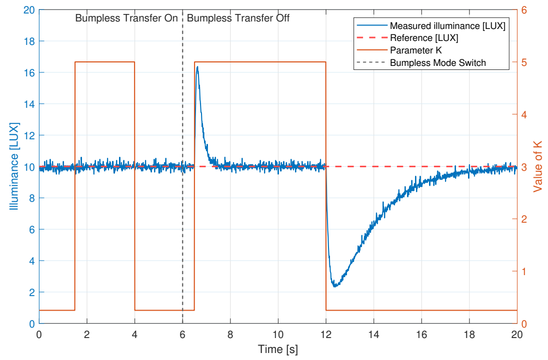

(b) Bumpless results (Left - ON / Right - OFF)

Figure 11

5.3 Characterizing Jitter and Process Time: Control, Serial, and Other Computations

To sample every $10ms$, a periodic task based on timer interrupts was used. The jitter associated is represented in the figure 12, where it can be seen that the maximum value between samples was $13\mu s$. Whenever a sample takes more time than expected, the subsequent one takes the same amount of extra time but in the opposite direction, indicating that no drift occurs. In other words, no additional delay occurs due to preceding samples being taken later than expected. Additionally, the time taken by some processes was measured and the average of each is displayed in the Table 5.

Process	Time [μs]
Digital Filter	130.1627
PID controller	29.3043
Calculate metrics and store buffer	15.8792
Serial Print of 3 variables	287.2427

Table 5: Time taken by some processes

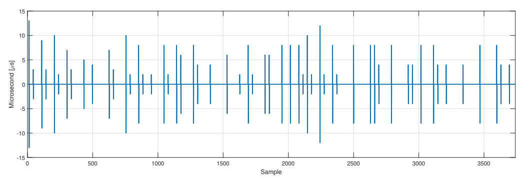

Figure 12: Time between samples

5.4 Performance metrics

This work focuses on user comfort while minimizing energy consumption. To evaluate its performance, specific metrics have been developed. These metrics include flicker error and visibility error, which prioritize the user experience, as well as energy consumption, which assesses the efficiency of energy minimization efforts. All metrics represented in the figure 13 were measured while doing the response to the steps shown on the figure 9b. In Figure 13b, it is important to consider values only after stabilization, disregarding transition phases. Considering that, all metrics demonstrated great results.

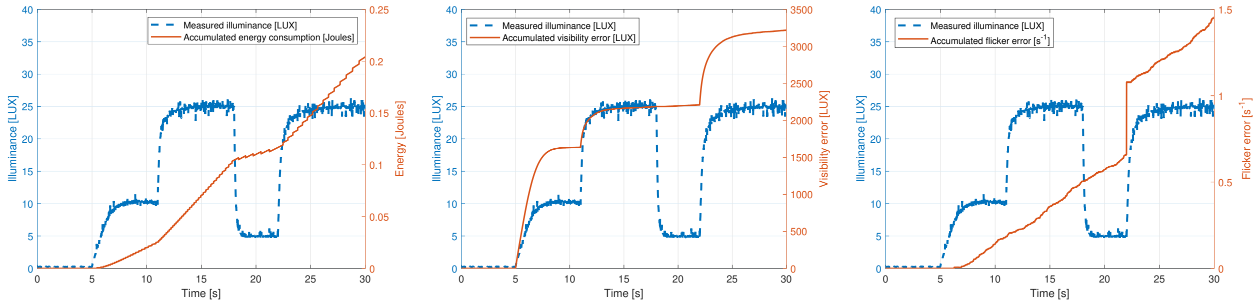

(a) Energy consumption **(b)** Accumulated visibility error **(c)** Accumulated flicker error

Figure 13: Performance metrics

6 Commands

All the commands presented in the Table 1 and Table 2 of the project assignment were implemented. Additionally, the commands shown in the table 6 were also implemented.

Command	Request	Response	Comments
Set the parameter K of luminaire <i> to <val>	K <i><val>	'ack' or 'err	
Set the parameter b of luminaire <i> to <val>	b <i><val>	'ack' or 'err	
Get all the parameters of the PID luminaire <i>	g i <i>	"i <i> - h = <val1>, K = <val2>, b = <val3>, Ti = <val4>, Tt = <val5>, Td = <val6>, N = <val7>"	The parameters of the values specified.
Start/Stop a stream of useful data from luminaire <i>to help debugging	D <i>	"<ref_min> <ref_max> <val1> <val2> <val3>"	The ref min and ref max are values set at 0 and 40, respectively, to define the limits of the graphs on the Serial Plotter. <val1> represents the current illuminance value being read, measured in LUX, while <val2> corresponds to the reference illuminance value, also in LUX. <val3>indicates the duty cycle, ranging from 0 to 100.
Set the current occupancy state of desk <i>	o <i><val>	'ack' or 'err'	Added an option with a value of 2 to <val> that sets the luminaire to the off state.
Set bumpless state of desk <i>	l <i><val>	'ack' or 'err'	<val> is a Boolean flag: 0 – off, 1 – on.
Get the static gain of the desk <i>	g g <i>	g <i><val>	<val>is a floating point number that expresses the static gain of the desk <i> [LUX/DutyCycle]

Table 6: Extra commands

7 Conclusion

In this project, we explored the potential of a set-point weighting PI controller for implementing a luminaire capable of dynamically adjusting lighting levels. Additionally, we implemented several methods, such as anti-windup and bumpless transfer, to enhance the controller's performance further.

Overall, the results obtained in real-world scenarios were promising, demonstrating a strong response to changes in the reference.